

## Supporting Information

Remarkable proton conducting behavior driven by the synergistic effects in an acid base conjugated MOFs impregnated with sulphuric acid molecules

Lu Feng<sup>a,§</sup>, Shuyang Bian<sup>c,§</sup>, Kun Zhang<sup>b,\*</sup> and Hong Zhou<sup>a,\*</sup>

<sup>a</sup> College of Chemistry and Environmental Technology, Wuhan Institute of Technology, Wuhan 430073, Hubei, China.

<sup>b</sup> Automotive Engineering Research Institute, Jiangsu University, 301 Xuefu road, Zhenjiang 212013, P. R. China.

<sup>c</sup> School of Chemistry and Chemical Engineering, Nanjing University of Science and Technology, Nanjing, Jiangsu 210094, China.

<sup>§</sup> These authors contributed equally to this work.

\* Corresponding Authors: [hzhoub@126.com](mailto:hzhoub@126.com) (H. Zhou); [zh198958@126.com](mailto:zh198958@126.com) (K. Zhang)

Table S1. Elemental analysis for  $\text{UiO-66-SO}_3^- \text{-NH}_3^+$

Sample	N(%)	C(%)	H(%)	S(%)
$\text{UiO-66-SO}_3^- \text{-NH}_3^+$	2.62	27.73	2.55	3.26

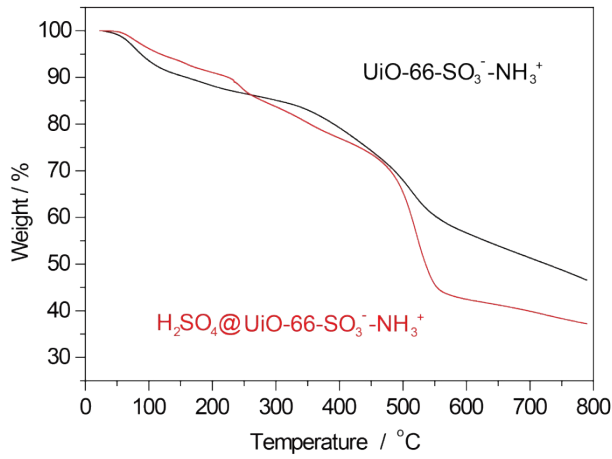


Fig. S1. TG plots of  $\text{UiO-66-SO}_3^- \text{-NH}_3^+$  and  $\text{H}_2\text{SO}_4 @ \text{UiO-66-SO}_3^- \text{-NH}_3^+$ .

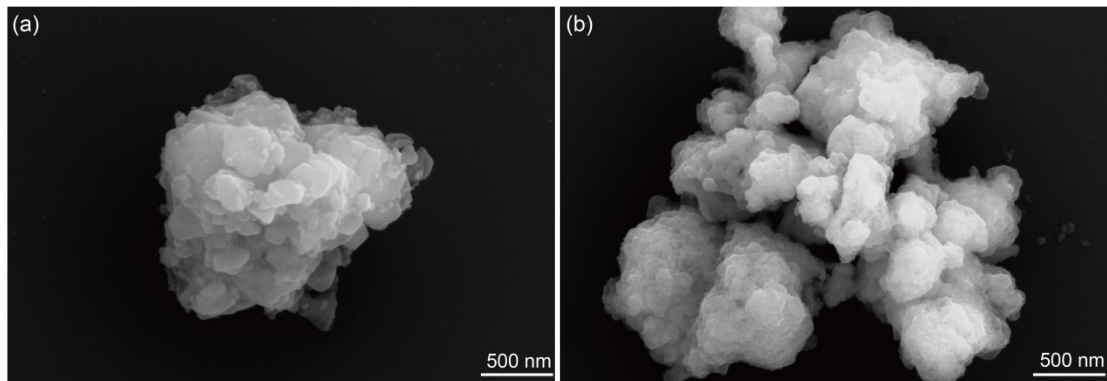


Fig. S2. SEM of composites: (a) for  $\text{UiO-66-SO}_3^- \text{-NH}_3^+$  and (b) for  $\text{H}_2\text{SO}_4 @ \text{UiO-66-SO}_3^- \text{-NH}_3^+$ .

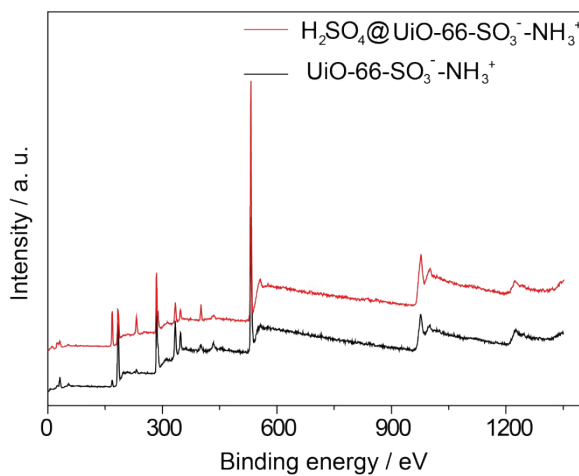


Fig. S3. XPS of  $\text{UiO-66-SO}_3^- \text{-NH}_3^+$  and  $\text{H}_2\text{SO}_4 @ \text{UiO-66-SO}_3^- \text{-NH}_3^+$ .

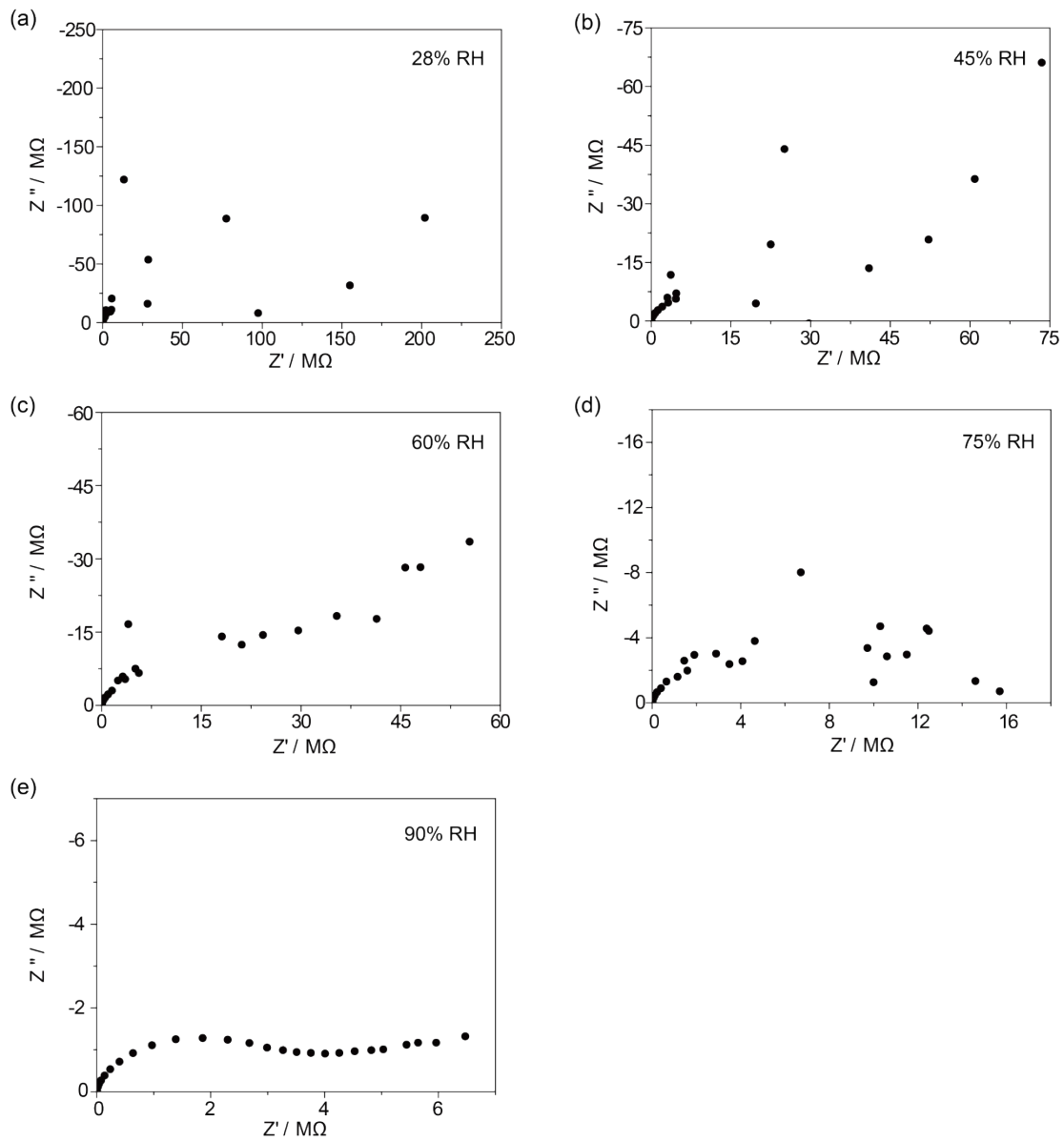


Fig. S4. Nyquist plots of  $\text{UiO-66-SO}_3^-\text{-NH}_3^+$  at  $30\text{ }^\circ\text{C}$  and different relative humidity.

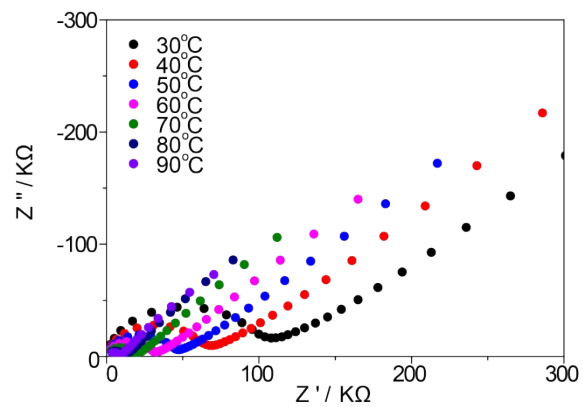


Fig. S5. Nyquist plots of  $\text{UiO-66-SO}_3^-\text{-NH}_3^+$  versus different temperature at 100% RH.

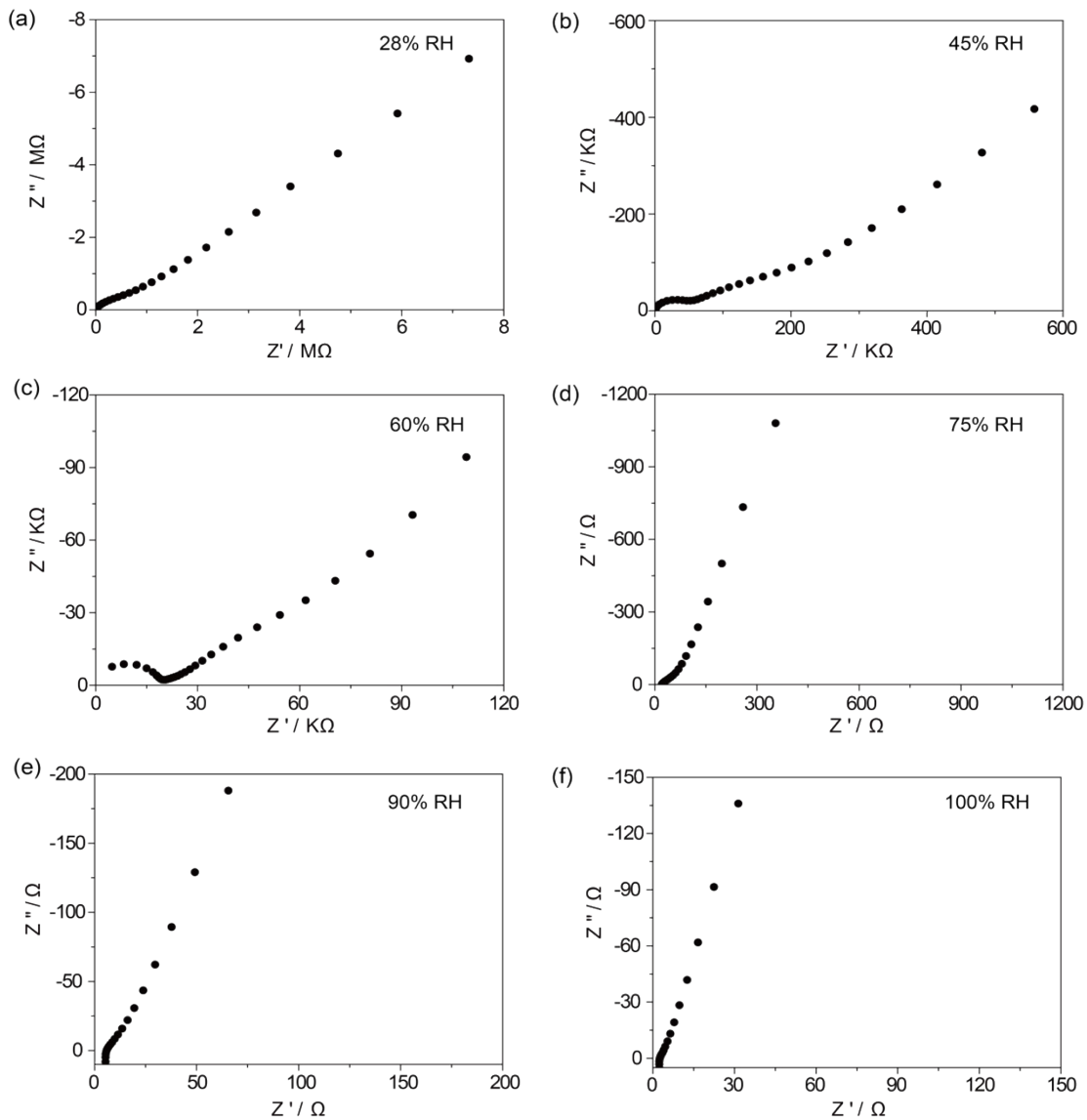


Fig. S6. Nyquist plots of  $\text{H}_2\text{SO}_4@\text{UiO-66-SO}_3^-\text{-NH}_3^+$  versus different relative humidity at 30 °C.

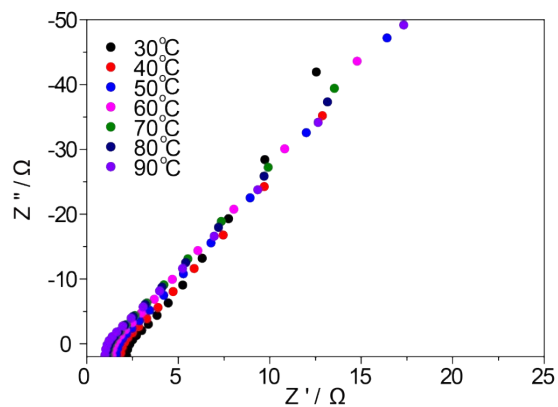


Fig. S7. Nyquist plots of  $\text{H}_2\text{SO}_4@\text{UiO-66-SO}_3^-\text{-NH}_3^+$  versus different temperature at 100% RH.

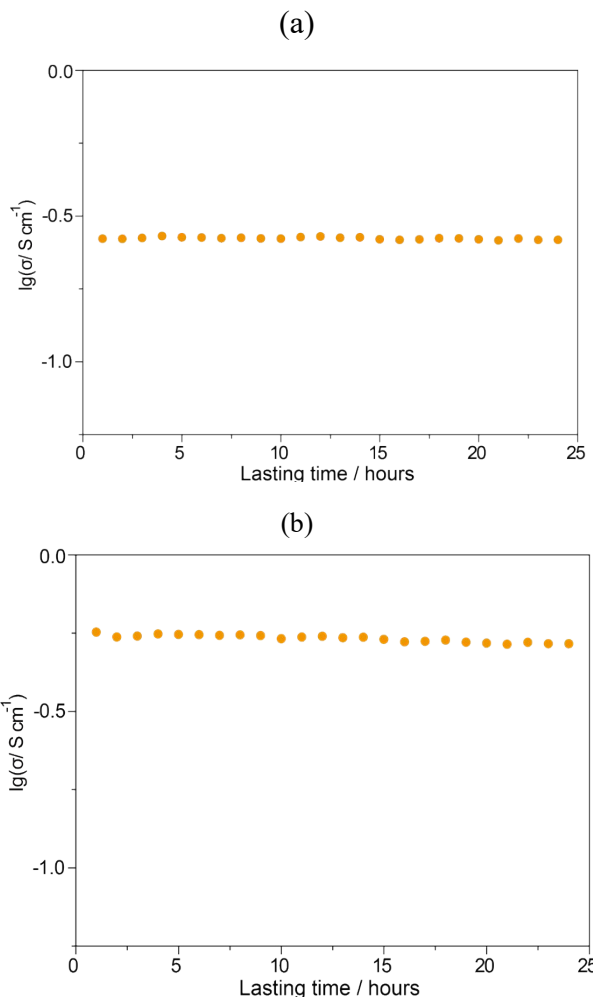


Fig. S8. Long-term proton conducting durability measurement of  $\text{H}_2\text{SO}_4@\text{UiO-66-SO}_3^-\text{NH}_3^+$  at 100% RH and 30 °C (a) as well as 90 °C (b).

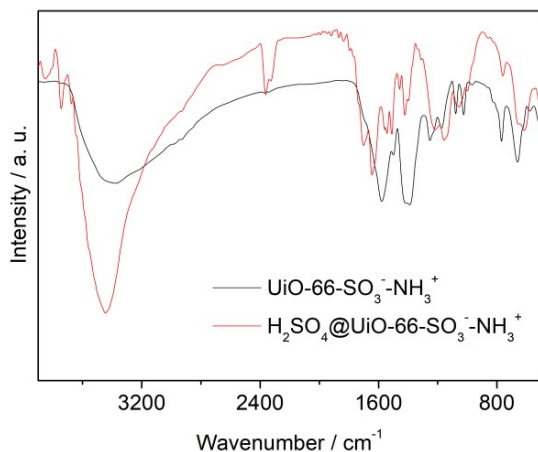


Fig. S9. Complete IR spectra of  $\text{H}_2\text{SO}_4@\text{UiO-66-SO}_3^-\text{NH}_3^+$  and  $\text{UiO-66-SO}_3^-\text{NH}_3^+$ .

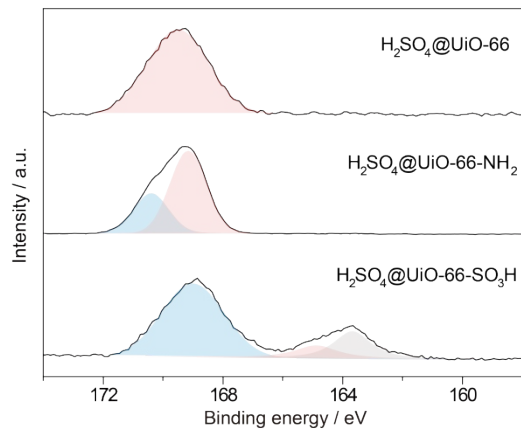


Fig. S10. S binding energy of  $\text{H}_2\text{SO}_4@\text{UiO-66}$ ,  $\text{H}_2\text{SO}_4@\text{UiO-66-NH}_2$  and  $\text{H}_2\text{SO}_4@\text{UiO-66-SO}_3\text{H}$ .

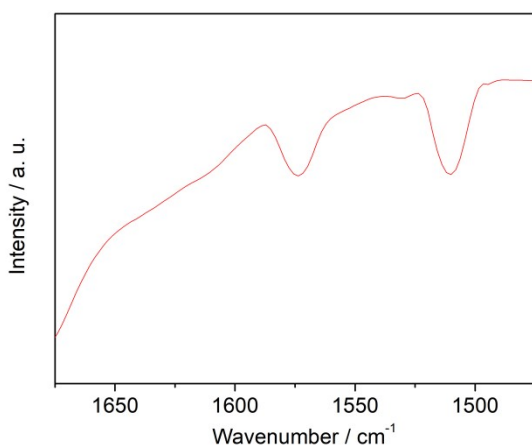


Fig. S11. IR spectrum of  $\text{H}_2\text{SO}_4@\text{UiO-66}$ .

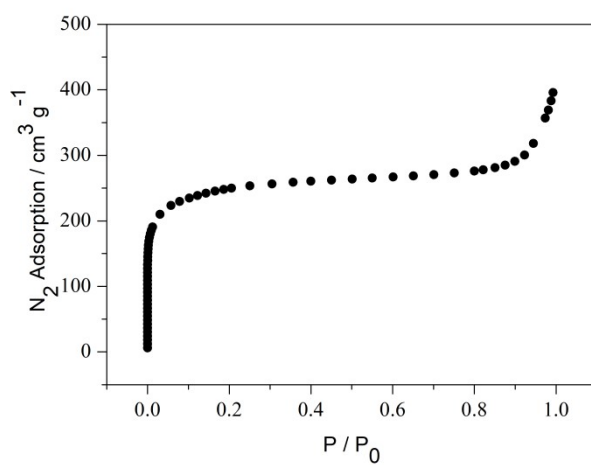


Fig. S12. Nitrogen adsorption of washed  $\text{H}_2\text{SO}_4@\text{UiO-66-SO}_3^-\text{NH}_3^+$ .

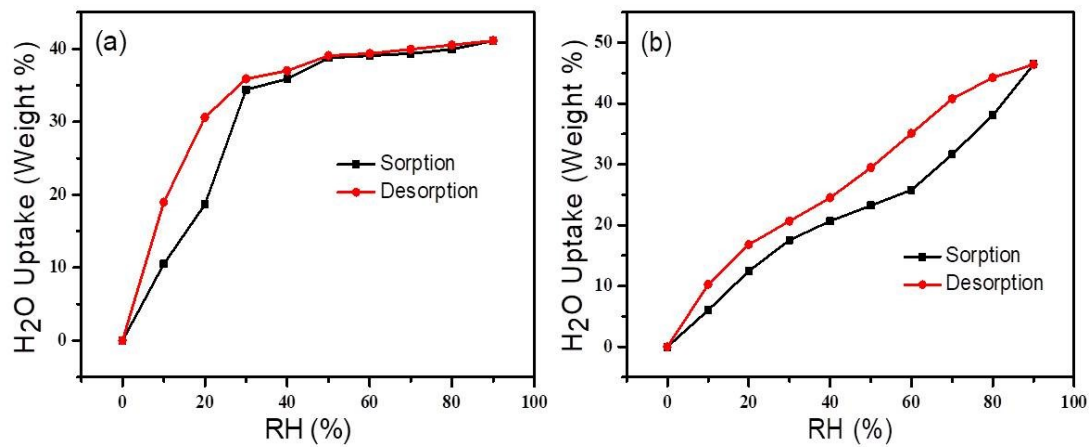


Fig. S13 Water adsorption–desorption isotherms of  $\text{UiO-66-SO}_3^-\text{-NH}_3^+$  (a) and  $\text{H}_2\text{SO}_4@\text{UiO-66-SO}_3^-\text{-NH}_3^+$  (b) measured at  $25\text{ }^\circ\text{C}$ .